

Surface-shifted core levels in Mo₃Si (100) and (110)

L. I. Johansson, K. L. Håkansson, and P. L. Wincott*

Department of Physics and Measurement Technology, Linköping University, S-58183 Linköping, Sweden

U. O. Karlsson

MAXLAB, Box 118, University of Lund, S-22100 Lund, Sweden

A. N. Christensen

Department of Chemistry, Aarhus University, DK-8000 Aarhus C, Denmark

(Received 2 November 1990)

High-resolution photoemission studies of core levels in Mo₃Si have been carried out using synchrotron radiation. Surface-shifted Si 2*p* components were observed on annealed (100) and (110) crystal faces and were unambiguously identified in adsorption experiments of hydrogen and oxygen. The surface core-level shifts were extracted using a curve-fitting procedure. For the (110) surface one shifted component was identified having a surface shift of $-1.02(1)$ eV. For the (100) surface two shifted components were found to be necessary in order to model the experimental spectrum, the stronger component having a shift of $-0.68(2)$ eV and the weaker a shift of $-1.03(4)$ eV. No surface-shifted components could be identified in the Mo 4*p* photoelectron spectrum. Upon oxygen adsorption a chemically shifted Si 2*p* component was observed, indicating silicon oxidation, while no chemically shifted component appeared in the Mo 4*p* spectrum. In the Si 2*p* spectrum pronounced photoelectron-diffraction effects were observed both as a function of photoelectron kinetic energy and emission angle. These findings are presented and discussed.

I. INTRODUCTION

The importance of metal silicides to semiconductor technology¹ has promoted extensive study of the electronic and structure properties of silicide surfaces and metal-silicon interfaces. Most investigations of silicide surfaces have been carried out on thin films or samples reacted *in situ*, and relatively few have been made on bulk silicide crystals. In this paper we present results from core-level photoemission studies of the refractory metal silicide Mo₃Si. Refractory metal-silicon interfaces have received a great deal of attention² and detailed investigations have been carried out³⁻⁸ focusing on the growth mode and possible intermixing in the interface region, silicide formation, and the characterization of the electronic densities in the few first interface layers. At room temperature a layer-by-layer growth without mixing of Mo onto Si(111)(7×7) was reported,^{3,4} while for the Si(111)(2×1) surface a considerable Mo-Si intermixing in the early growth of the interface was observed⁵⁻⁷ and interpreted as formation of islands of silicides having a preferential stoichiometry. Annealings have been shown to favor material intermixing and for adsorbed Mo layers on the Si(111)(7×7) surface annealings to $T > 500^\circ\text{C}$ were found to produce homogeneous and stable MoSi₂ (Refs. 3 and 4) while for the counterpart system, Si layers adsorbed on polycrystalline Mo, annealings were found to give rise to mixed layers in which the Si concentration decreased with temperature.⁸ Results from electronic-structure studies of *in situ* fractured bulk refractory metal disilicides⁹ were used in these interpretations. Characterization of different refractory metal silicide bulk crystals

therefore seems well motivated since it may provide information of importance also for interpreting metal-silicon interface reactions. Questions have been raised concerning the nature of the terminating layer, the stoichiometry and silicon bonding configuration. For MoSi₂(100) it was shown¹⁰ in a recent investigation that the surface, which was prepared by *in situ* cleaving, was terminated by a Si monolayer.

We have performed angle-resolved photoemission studies of Mo₃Si(100) and Mo₃Si(110) using synchrotron radiation for the purpose of elucidating the electronic and structure properties of these surfaces. Below we present results obtained in high-resolution core-level studies of the clean surfaces, prepared *in situ* by sputter and annealing cycles. Results of valence-band studies are planned to be presented separately.¹¹ For both surfaces investigated the core-level spectra reveal surface shifted Si 2*p* levels while no surface-shifted Mo 4*p* component can be observed. The effects induced in the core-level spectra upon oxygen (and hydrogen) exposures allow an unambiguous identification of the surface-shifted components. These effects moreover indicate a rapid oxidation of Si while, even at the largest exposures investigated, no effect was observed in the Mo 4*p* spectrum. The surface-to-bulk Si 2*p* intensity ratio extracted at different photon energies and also at different electron emission angles show pronounced diffraction effects. These results are presented and discussed below.

II. EXPERIMENT

The experiments were performed at the synchrotron radiation facility MAX laboratory using a beam line

equipped with a toroidal grating monochromator¹² and an angle-resolved photoelectron spectrometer (Vacuum Science Workshop). The monochromator has three interchangeable gratings and covers the photon range 20–200 eV. The photon energy resolution is dependent on the operating parameters but was for the high-resolution studies of the Si $2p$ levels typically chosen to be <0.2 eV. The hemispherical electron analyzer has an acceptance angle of $\pm 2^\circ$ and was normally operated at an energy resolution of 0.15 eV. The base pressure in the spectrometer was $<2 \times 10^{-10}$ Torr.

Mo_3Si melts incongruently.¹³ However, single crystals of Mo_3Si can be grown by a modified floating-zone procedure, the so-called traveling-solvent growth method. In this procedure the molten zone of solvent has the nominal composition Mo_4Si , and the feed rod and grown crystal the composition Mo_3Si . The volume of the zone of solvent must be kept constant during the growth process. The crystals of Mo_3Si were made in an ADL-MP crystal growth unit in an ambient He pressure of 2 MPa, using a growth rate of 1 mm h^{-1} .

Two smaller crystals having the (100) and (110) orientation were spark cut from this monocrystal. These crystals were mechanically polished and the orientation was checked to be within $\pm 1^\circ$ by means of Laue patterns. They were then mounted and cleaned *in situ*. A short Ar^+ -ion bombardment (ca. $1 \mu\text{A}$ at 600 V for 5 min) is needed initially and is then followed by repeated annealings. For the (100) surface an annealing temperature of about 900°C , and for the (110) surface a temperature of about 750°C , was found necessary to produce a well-ordered surface. The surface cleanliness and order was checked by Auger electron spectroscopy (AES) and low-energy electron diffraction (LEED) and after cleaning a distinct 1×1 LEED pattern was observed from both surfaces. Changes in the surface composition during the cleaning procedure had been monitored¹¹ using AES and after a few annealings a constant ratio between Si and Mo peak heights was obtained and observed not to change upon repeated annealings. Valence-band and core-level photoemission spectra recorded after cleaning and annealing cycles confirmed this behavior and also showed a constant surface-to-bulk peak ratio. The LEED pattern was utilized to set the desired azimuthal direction for the crystal under investigation. The incidence and emission angles are given below relative to the surface normal and the energies are referenced to the measured Fermi level. All measurements were performed at room temperature. Gas exposures were made at pressures in the 10^{-8} – 10^{-5} Torr range and the exposure is given as the total pressure read on the ion gauge times the exposure time ($1\text{L} = 10^{-6}$ Torr s). During hydrogen exposures the sample was facing a hot (1700°C) tungsten filament in order to produce activated hydrogen.

III. RESULTS

High-resolution Si $2p$ spectra recorded from the (100) and (110) surface at normal emission using a photon energy of 117 eV are shown by the dotted curves in Figs. 1(a) and 1(b). In neither of these is only a simple spin-split Si

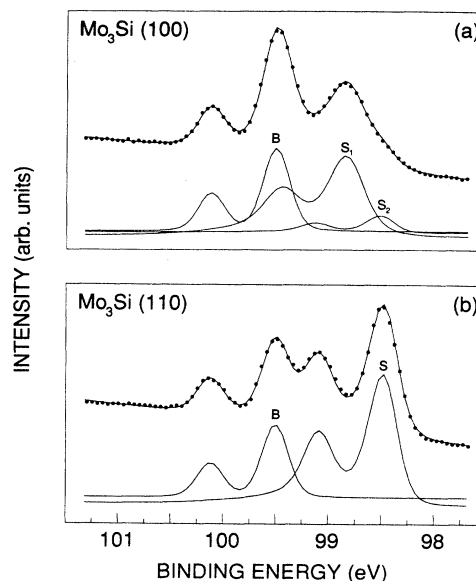


FIG. 1. Si $2p$ core-level spectra recorded at normal emission from (a) the (100) surface and (b) the (110) surface using a photon energy of 117 eV. The dotted curve shows the recorded data points, the solid curve represents the result of the curve-fitting procedure and the bottom curves show the extracted bulk (B) and surface-shifted (S) components.

$2p$ doublet observed. Instead the spectra are seen to contain contributions from two or three components, which are identified below as bulk- and surface-shifted components, respectively. These components were extracted using a curve-fitting procedure.¹⁴ For the (110) spectrum a single surface-shifted Si $2p$ component was found to produce fairly good fits while for the (100) spectrum two surface-shifted Si $2p$ doublets were found to be needed in order to model the experimental results. The bottom curves in Figs. 1(a) and 1(b) show the extracted components and the solid curves through the data points show the fitted curves. The surface-shifted components are identified below. For the (110) surface the surface component has a shift of $-1.02(1)$ eV, where the value specified in the parentheses represents the uncertainty in the last digit. For the (100) surface the strongest surface component has a shift of $-0.68(2)$ eV while the weaker component has a shift of $-1.03(4)$ eV. Efforts to fit the (100) spectrum using only one surface component produced fits of poorer quality. The asymmetry that the lower binding energy peak exhibits, see Fig. 1(a), could not be modeled properly using only one surface-shifted component. In the fitting procedure it was assumed that the spin-orbit splitted peaks can be represented by asymmetric Lorentzian peak profiles convoluted with a Gaussian broadening function. The spin-split peaks were assumed to have the same halfwidth but the spin-orbit splitting, the asymmetry parameter, the Lorentzian width, and branching ratio of the bulk and surface components, respectively, were treated as independent parameters. The values of the fitting parameters found to

TABLE I. Parameters used in the curve-fitting and extracted surface core-level shifts (SCLS). The extracted surface core-level shifts are given as the arithmetic average (and the spread in the last digit) of the shifts determined at the photon energies utilized between 114 and 165 eV. For the branching ratio a certain spread in the fitting parameter was allowed, a spread we think mainly arises from difficulties in modeling the background at low kinetic energies. FWHM represents full width at half maximum.

	Bulk	Surface 1	Surface 2
Lorentzian FWHM (eV)	0.07	0.10	0.10
Asymmetry parameter	0.00	0.12	0.12
Spin-orbit split (eV)	0.618	0.605	0.605
Branching ratio	0.50(1)	0.50(2)	0.50(1)
Gaussian FWHM (eV)			
at $h\nu=117$ eV	0.25	0.25	0.25
SCLS (eV) for (110) surface		-1.02(1)	
Surface-to-bulk			
ratio at $h\nu=117$ eV		1.9	
SCLS (eV) for (100) surface		-0.68(2)	-1.03(4)
Surface-to-bulk			
ratio at $h\nu=117$ eV		0.9	0.1

produce best fits are summarized in Table I together with the extracted surface core-level shifts. The core-level shifts were, however, found to be fairly insensitive to the fitting parameters used.

Since surface core-level shifts were observed in the Si 2*p* spectrum we also tried to resolve surface-shifted Mo levels, if any. For this purpose we investigated the Mo 4*p* levels which are considerably broader and weaker than the Si 2*p*. This is illustrated in Fig. 2 where a Mo 4*p* spectrum recorded at normal emission from the (100) surface using a photon energy of 100 eV is shown by the dotted curve. An analyzer pass energy of 25 eV instead of 10 eV was used in this case, which gives an additional instrumental broadening compared to the Si 2*p* spectrum. A single doublet with a spin-orbit splitting of 2.11 eV,

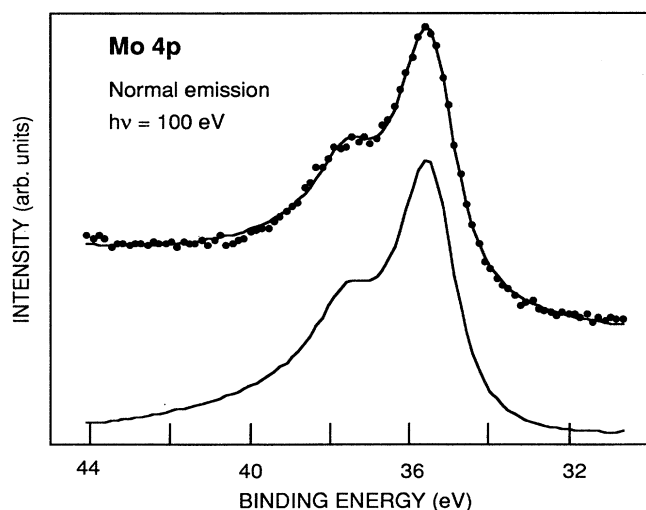


FIG. 2. Mo 4*p* core-level spectrum recorded at normal emission from the (100) surface using a photon energy of 100 eV. The experimental curve (dotted) is found to be modeled fairly satisfactory using a single doublet (solid curve) and no surface-shifted component can be identified.

which agrees well with the splitting of 2.1 eV observed in a previous investigation⁹ of MoSi₂, is found to reproduce the experimental curve quite well as shown by the solid curve in Fig. 2. For the fitted curve a branching ratio of 0.27, a Gaussian width of 0.45 eV, an asymmetry parameter of 0.23, and a Lorentzian width of 1.35 eV were utilized. In order to obtain a higher surface sensitivity the Mo 4*p* spectrum was also recorded at a large electron emission angle ($\theta_e = 50^\circ$) but no additional broadening could be resolved. The Mo 4*p* spectra recorded from the (110) surface were also very similar to the one shown in Fig. 2. We therefore conclude that there is no surface-shifted component in the Mo 4*p* spectrum.

Surface-shifted core levels are generally more sensitive to surface contamination than the corresponding bulk levels. Therefore, gas adsorption experiments were made in order to determine which of the components are the surface-shifted ones. The effects induced in the Si 2*p* spectrum upon hydrogen exposure are shown in Figs. 3(a) and 3(b), respectively, for the (100) and (110) surfaces. It is seen that the lower binding energy components are strongly affected by hydrogen exposures while the higher binding energy component remains essentially unaffected. The effect is clearly visible in both cases, although more pronounced in the (110) spectrum. We have no explanation for this difference. We could not observe any changes in peak positions upon hydrogen exposure but merely a decrease in intensity of the low binding energy components. The effects induced in the Si 2*p* spectrum upon oxygen exposure are, for the low binding energy components, similar to what was observed after hydrogen exposure. A decrease in intensity with increasing exposure, although more rapid in the oxygen case, as shown in Figs. 4(a) and 4(b). These observations following hydrogen and oxygen adsorption show unambiguously that the low binding energy components are the surface-shifted ones. Another interesting observation is made after oxygen exposures. Chemically shifted Si 2*p* levels appear at about 3 eV larger binding energy than the bulk peaks of the clean crystal, indicating oxidation of Si.¹⁵ This is al-

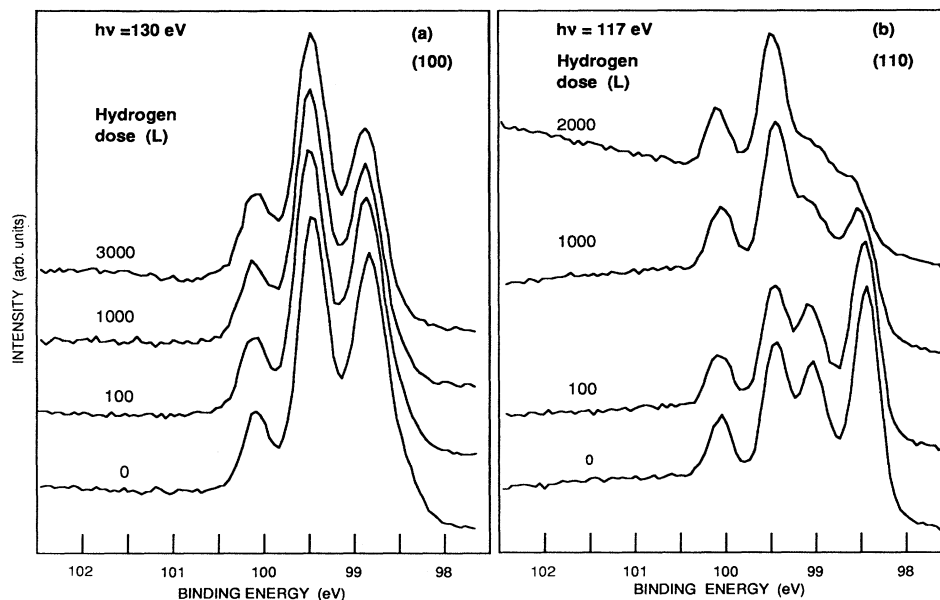


FIG. 3. Si 2*p* spectrum recorded at normal emission after different hydrogen exposures (a) from the (100) surface using a photon energy of 130 eV and (b) from the (110) surface using $h\nu=117$ eV (the change in background between the two largest exposures was caused by experimental adjustments and is not an effect of the exposure).

ready observed after an exposure of <10 L indicating that the Si on Mo_3Si appears more reactive towards oxygen than the Si on a pure Si surface.¹⁵ No chemically shifted Mo 4*p* component could be resolved after the largest oxygen exposure investigated, 5000 L, which is surprising but we believe this can be ascribed mainly to poor sensitivity since the Mo 4*p* levels are quite weak and broad compared to the Si 2*p* levels. These observations

are similar to those made earlier on V_3Si ,¹⁶ a rapid initial oxidation of Si and much slower V oxide growth, and they support the proposed ideas¹⁶ that O_2 chemisorbs dissociatively on transition-metal sites on the silicide and that a rapid O spillover to silicon sites occurs where oxidative attack ensues. It should be noted that after the largest hydrogen exposures a weak signal was observed at about 5 eV lower binding energy than the Mo 4*p*. We be-

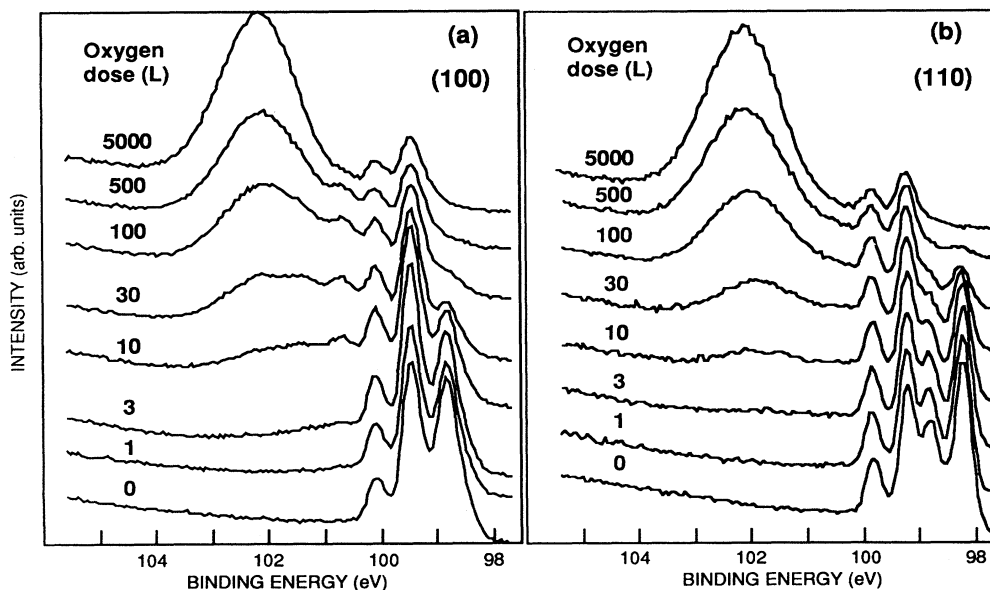


FIG. 4. Si 2*p* spectrum recorded at normal emission after different oxygen exposures using a photon energy of 130 eV, (a) from the (100) surface and (b) from the (110) surface.

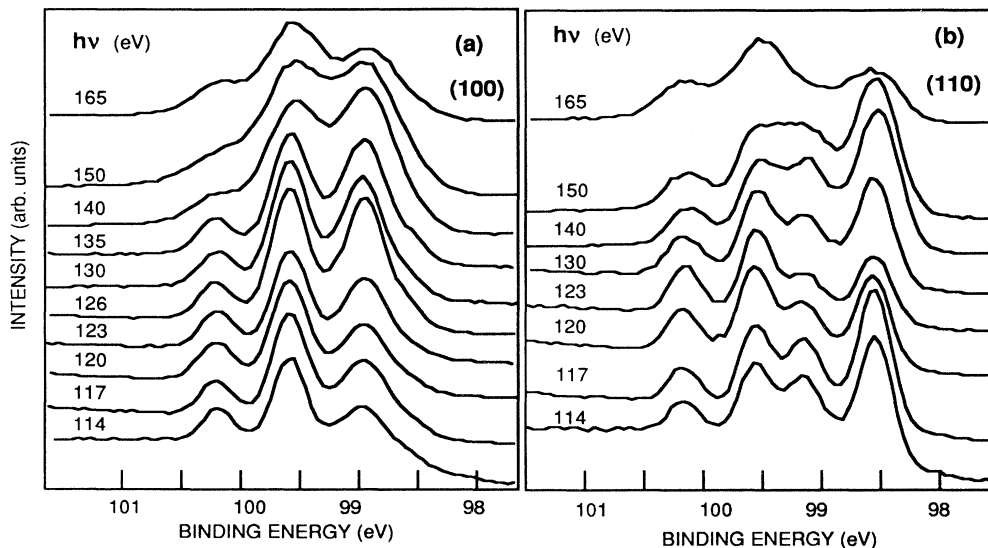


FIG. 5. Si $2p$ spectrum recorded, using different photon energies, at normal emission from (a) the (100) surface and (b) the (110) surface.

lieve that this structure may originate from As $3d$, i.e., from As contamination transported to the surface from the system walls by the activated hydrogen gas. No such structure was observed after oxygen exposures or after exposing the surface only to the hot filament for a few minutes.

For the purpose of observing whether the intensity ratio between surface and bulk Si $2p$ peaks would vary in the simple manner expected from the variation in electron probe depth, the Si $2p$ spectrum was studied both as a function of photon energy and as a function of electron emission angle. Since the electron inelastic mean free path is generally considered to follow the behavior predicted by the universal curve¹⁷ the intensity ratio versus photon energy is expected to vary smoothly and show a

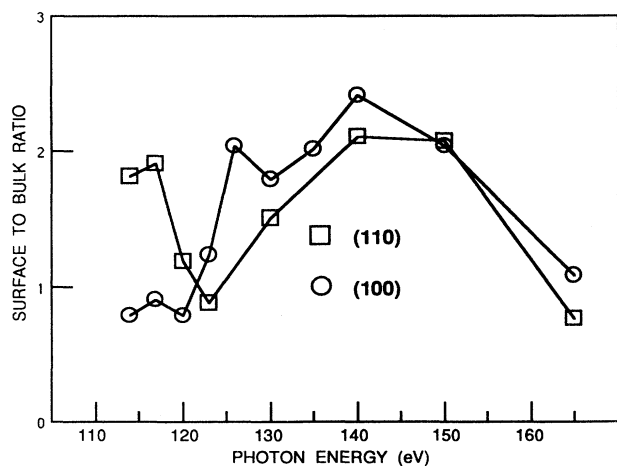


FIG. 6. Surface-to-bulk intensity ratio determined as a function of photon energy.

maximum at an energy where the mean free path is smallest. In a study of Cl adsorbed on Si(111) at saturation coverage, where one layer of Si atoms, each bonded to a Cl atom, is formed, the surface-to-bulk Si $2p$ peak ratio was shown to vary fairly monotonically and to exhibit a maximum at a kinetic energy corresponding to a photon energy around 130 eV.¹⁸ Normal emission Si $2p$ spectra recorded from the (100) and (110) surface using photon energies between 114 and 165 eV are shown in Figs. 5(a) and 5(b). For the (100) surface the peak height ratio between the surface and bulk components is, in Fig. 5(a), seen to vary fairly smoothly and show a maximum at a photon energy around 140 eV. For the (110) surface, however, the ratio shows a different behavior, see Fig. 5(b). The ratio is high at the two lowest photon energies, it then decreases showing a minimum at a photon energy of 123 eV followed by an increase to a maximum around 140 eV and then decreases with increasing photon energy. In order to quantify the variation in relative intensity between the bulk- and surface-shifted components the curve-fitting procedure was used to extract the peak areas. Since the photon energy resolution decreases with increasing energy the Gaussian broadening parameter was optimized at each photon energy. The other parameters were, however, selected to be the same when extracting the peak areas. For the (100) surface we consider only the ratio between the major surface-shifted component and the bulk component and neglect the weaker one, whose peak area typically was $< 10\%$ of the major component. The peak area ratio determined between the surface and bulk peaks is plotted versus photon energy in Fig. 6. These ratios show, for the (110) surface, that photoelectron diffraction effects do play an important role since the behavior with photon energy is very different from the expected variation in electron probing depth.

The Si $2p$ spectrum was also investigated as a function

of electron emission angle θ_e . The surface-to-bulk intensity ratio is predicted to increase monotonically with increasing emission angle¹⁹ if photoelectron diffraction effects are neglected. Spectra recorded at different emission angles using a photon energy of 123 eV are shown in Figs. 7(a) and 7(b), respectively, for the (100) and (110) surface. The azimuthal direction was for the (100) surface along the $\langle 011 \rangle$ direction and for the (110) surface along the $\langle \bar{1}10 \rangle$ direction. The curve-fitting procedure was used to extract the peak area of the surface and bulk components. In this case only the position and relative peak intensities were allowed to vary when fitting the curves for a particular photon energy. In Figs. 8(a) and 8(b) the peak area ratio extracted between the surface and bulk peaks is plotted versus electron emission angle for three different photon energies. Concentrating first on

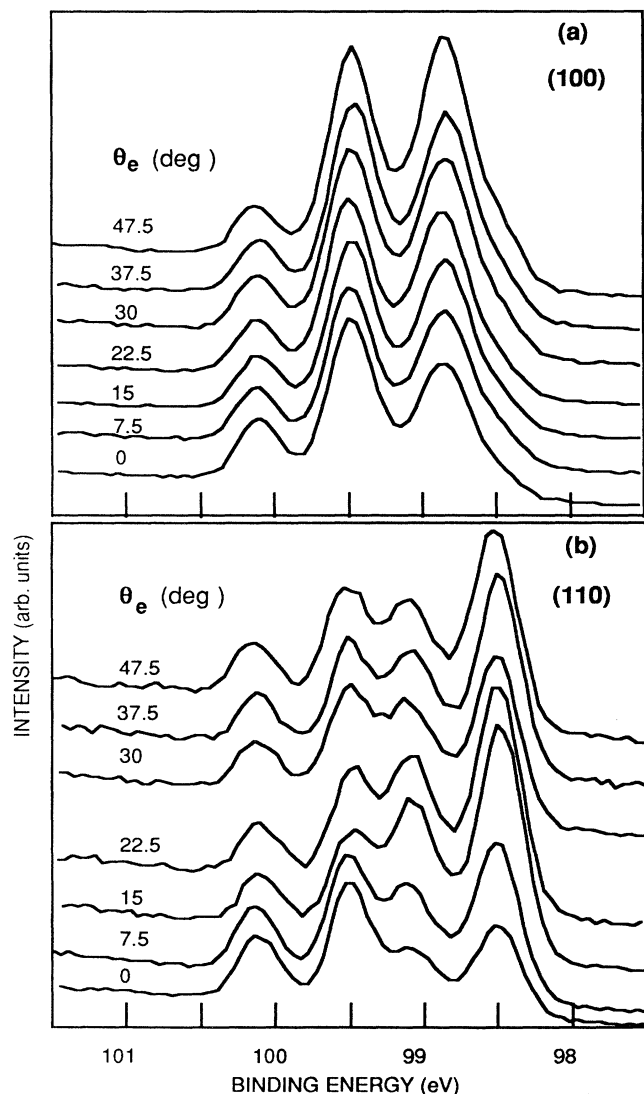


FIG. 7. Si 2p spectrum recorded at different emission angles from (a) the (100) surface and (b) the (110) surface using a photon energy of 123 eV.

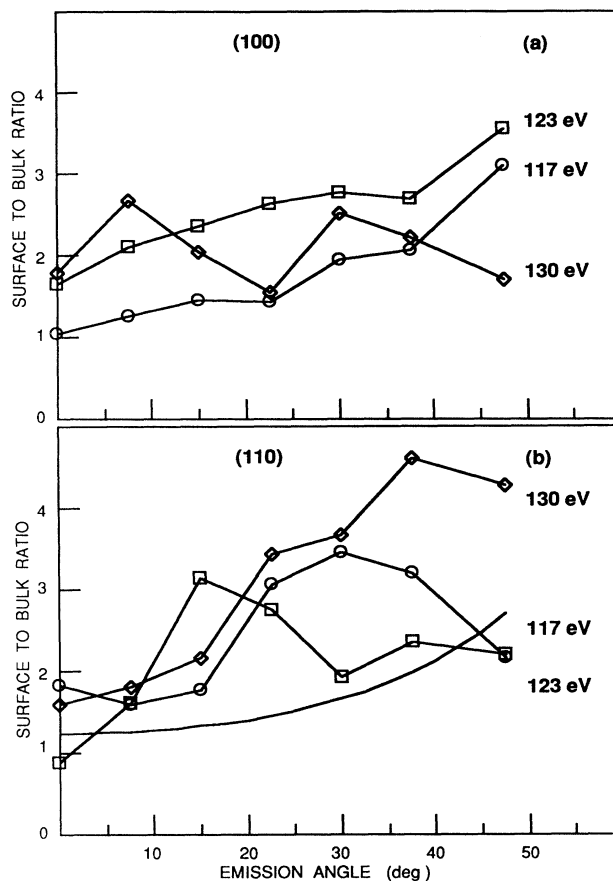


FIG. 8. Surface-to-bulk intensity ratio determined as a function of electron emission angle from (a) (100) along the $\langle 011 \rangle$ azimuth and (b) (110) along the $\langle \bar{1}10 \rangle$ azimuth. The intensity ratio has been determined at three different photon energies.

the results obtained at $h\nu=123$ eV, distinct differences are observed between the (100) and (110) results. From the (100) surface, Figs. 7(a) and 8(a), a monotonic increase of the surface-to-bulk peak area ratio with increasing emission angle is observed, as expected if diffraction effects could be neglected. For the (110) surface, however, Figs. 7(b) and 8(b), the largest peak area ratio is observed at an emission angle of $\theta_e=15^\circ$. At the two other photon energies used the variation in peak area ratio with emission angle is seen to be different, see Fig. 8, but in some of these cases the largest ratio does not correspond to the largest emission angle investigated. These observations of maxima in the peak area ratio at intermediate angles clearly indicate that photoelectron diffraction effects play an important role and cannot be neglected in studies of these surfaces.

IV. DISCUSSION

Surface-shifted core levels were observed on both the surfaces investigated but their magnitudes were found to be different. The values specified above for the extracted core-level shifts of, respectively, $-0.68(2)$ and $-1.03(4)$

eV for the (100) surface and $-1.02(1)$ eV for the (110) surface actually represent the arithmetic average of the shifts determined at the photon energies utilized between 114 and 165 eV. The uncertainties given in parentheses represent the spread in the extracted values. These observations immediately cause some questions. Why is the shift negative and why is it larger in magnitude on the (110) surface than on the (100) surface?

An estimate of the surface core-level shift can be obtained from equations derived using the thermochemical model.^{20,21} However, since we are concerned with the solid compound, Mo₃Si, the equations of core-level shift derived for dilute solid solutions²¹ cannot be considered to be applicable. The most appropriate model is therefore the one in which the total shift is expressed as a sum of partial shifts.²⁰ The partial shift originating from the loss of coordination at the surface is in this model²⁰ given

$$\Delta E_v = c_v^* (E_{\text{coh}}^{z^*} - E_{\text{coh}}^z),$$

where c_v^* is an effective concentration parameter that quantifies the lack of coordination of the core ionized site at the surface compared to the bulk and $E_{\text{coh}}^{z^*}$ and E_{coh}^z , respectively, are the cohesion energies of the z^* and z solid (where z^* denotes a z metal with one core electron removed and one valence electron added). Tabulated values of the heat of formation²² for Mo₃Si and Mo₃P give a difference in cohesion energy of -0.42 eV. Thus the shift is expected to be negative but the value estimated for complete loss of coordination ($c_v^* = 1$) is considerably smaller than the experimentally observed shifts. The c_v^* parameter can to a first approximation be estimated²⁰ from the number of missing nearest-neighbor atoms at the surface compared to the bulk. Mo₃Si crystallizes in the *A15* structure (see Fig. 9) and in the bulk an Si atom has twelve nearest-neighbor Mo atoms (at a distance of $a\sqrt{5}/4$). Since the precise atomic arrangement at the surface has not been determined (relaxation and/or reconstruction effects may be present) the actual number of nearest neighbors of a surface Si atom is not known. In order to obtain an estimate, however, it seems reasonable to assume perfect bulk termination, although we suspect that Si may be enriched on the surface. The atomic arrangement for perfect bulk termination of the two surfaces is illustrated in Figs. 9(b) and 9(c). The (100) surface layer can consist of either a mixed layer of Si and Mo atoms or a pure Mo layer while the (110) surface layer can consist of either Si or Mo atoms. We have, in Figs. 9(b) and 9(c), assumed that the (100) surface is terminated by a mixed layer and that the (110) surface is Si terminated. A surface Si atom on the (100) surface then has eight nearest-neighbor Mo atoms (i.e., $c_v^* \approx 0.33$) and on the (110) surface this is reduced to six (i.e., $c_v^* \approx 0.5$). Thus the greater decrease in coordination number on the (110) surface can explain why the surface shift on the (110) surface is 50% larger than on the (100) surface. The magnitude of the observed shift is however much larger than the estimated value and therefore one may speculate about other contributions to the shift, surface chemical effects, for example.

It may be possible for a silicide of a different

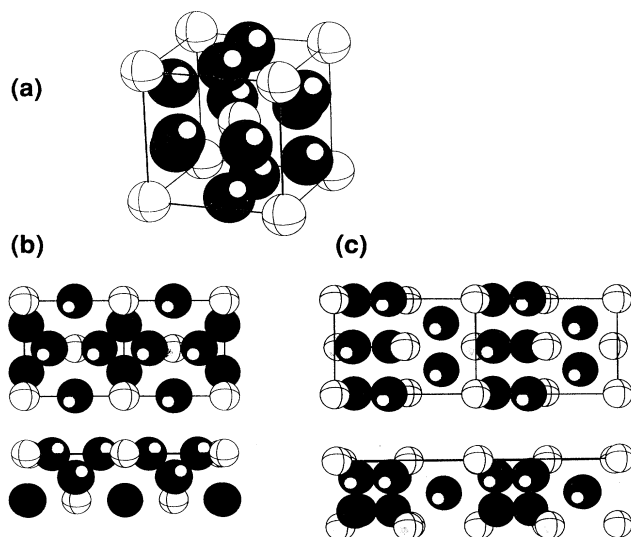


FIG. 9. (a) Unit cell of Mo₃Si, where open circles represent Si atoms and shaded circles Mo atoms. (b) Top and side view of the (100) surface when assuming perfect bulk termination and a surface layer containing both Si and Mo atoms. (c) Top and side view of the (110) surface when assuming perfect bulk termination by a Si surface layer.

stoichiometry to form in the surface region, e.g., MoSi or MoSi₂, thus giving rise to the shifted peak. For that to be the case the Si $2p$ binding energy should show a stoichiometry-dependent chemical shift of appreciable magnitude. The binding energy of the bulk Si $2p_{3/2}$ level in Mo₃Si was determined to be $99.5(1)$ eV which is close to the values previously observed for bulk MoSi₂ (Ref. 9) and reacted (as well as unreacted) Si-Mo interfaces⁸ and this therefore cannot explain the large shifts observed. From the effects induced in the core-level spectra upon oxygen (and hydrogen) exposures, a rapid attenuation of the shifted Si $2p$ components but no detectable effects in the Mo $4p$ spectrum, it seems reasonable to assume Si termination of these surfaces. Other recent studies on bulk CoSi₂, FeSi₂, and MoSi₂ surfaces, either fractured *in situ* or cleaned *in situ* by ion bombardment and annealing cycles, show that the surfaces in general are Si terminated.^{10,23,24} Earlier studies on epitaxially grown CoSi₂ thin films on Si(111) surfaces showed that the silicide surface may be terminated by one Co layer or one, two, or three Si layers dependent on growth conditions and post-growth treatments. For these bulk disilicides, however, the most recent results^{10,23-25} show that the surfaces are terminated by a single Si layer but they also show that sputtered annealed surfaces tend to be Si rich compared to cleaved surfaces. The enrichment may be caused by diffusion of Si atoms to the surface during the annealing process. In order to verify if this is the case for our Mo₃Si surfaces the amount of Si in the surface region has to be determined since we could not prepare cleaved surfaces. That the (110) surface of Mo₃Si can be Si terminated is easily understood since perfect bulk termination ei-

ther exposes a Si or Mo surface layer. The stacking sequence of these layers is illustrated in Fig. 9(c). Consecutive Si layers are separated by $a/\sqrt{2}$ and have three Mo layers in between. For the (100) surface perfect bulk termination either exposes a mixed layer or a Mo layer, see Fig. 9(b), and consecutive layers are separated by $a/2$. Perfect bulk termination for the (110) and (100) surface, resulting in Si and mixed layer termination, respectively, would give rise to differences in the surface-to-bulk intensity ratio that in principle should be possible to model. The surface-to-bulk intensity ratio R as a function of the electron emission angle θ is, when diffraction effects are neglected, given by¹⁹

$$R(\theta) = \exp(d/\lambda \cos\phi) - 1,$$

where d is the interlayer separation, λ is the energy-dependent mean free path, and ϕ is the emission angle within the crystal. The emission angle in vacuum θ is related to ϕ by

$$(1 + V_0/E_k)^{1/2} \sin\phi = \sin\theta,$$

where V_0 is the inner potential and E_k is the kinetic energy of the photoelectron in vacuum. The parameters θ and E_k are determined experimentally and by fitting to the experimental data it should, in principle, be possible to extract values for V_0 and λ that could be used to predict the ratio expected for the two surfaces. This model predicts a monotonically increasing ratio with increasing emission angle. The ratio calculated for the (110) surface for a mean free path of 4.3 Å,¹⁰ corresponding to a photon energy of about 130 eV ($E_k \approx 25$ eV), and an inner potential of 10 eV is shown in Fig. 8(b). The ratios determined for the (110) surface at different kinetic energies behave quite differently, however, as seen in Fig. 8(b). For pure Ge (100) the surface-to-bulk ratio showed¹⁹ a general increasing trend for increasing θ but with superimposed aperiodic oscillations, of up to 10%, due to diffraction. Much more pronounced diffraction effects were observed in the surface to bulk Si $2p$ ratio for different CoSi₂ surfaces.²³ The ratio was found to be a strongly modulated function of both emission angle and photoelectron kinetic energy and it was concluded that there was no basis for using the simple model¹⁹ described above. This is also true concerning our results; diffraction effects seem to dominate the data. The determined surface-to-bulk ratios are not found to increase monotonically with emission angle, see Fig. 8, or to show the expected behavior¹⁸ with electron kinetic energy, looking in particular at the (110) results in Fig. 6. Therefore it is not meaningful to try to estimate the amount of Si on the surfaces using this simple model.

Although these diffraction effects make any simple interpretation impossible they have, on the other hand, been shown to have great potential, when combined with theoretical calculations, to supply valuable structural information.^{24,26,27} A full multiple scattering type of calculation is needed because of the low kinetic energies in-

involved. Such calculations were recently²⁴ reported for CoSi₂(111) and compared to photoelectron diffraction results and it was found that the model in which the surface layer is terminated by only one Si layer was favored. At present we cannot perform such calculations and extract the structural information contained in the recorded data. Extension of this work to a more detailed study of the energy- and angle-dependent diffraction effects, including model calculations, is in progress.

One question that we have not addressed is why are two shifted levels observed on the (100) surface while only one is clearly observed on the (110) surface. Since so little is known about the atomic arrangement at the surface of this silicide we presently prefer not to speculate about the origin of this second shifted peak. Instead further studies are in progress employing better energy resolution for the purpose of revealing finer details about these surface-shifted levels.

V. SUMMARY AND CONCLUSIONS

Results of high-resolution core-level photoemission studies of the Mo₃Si (100) and (110) surfaces, cleaned *in situ* by sputter annealing cycles, are reported. Surface-shifted Si $2p$ levels were revealed on both surfaces while no surface-shifted Mo $4p$ component could be detected. The effects induced in the core-level spectra upon oxygen (and hydrogen) exposures allowed an unambiguous identification of the surface-shifted components and they moreover showed that a rapid oxidation of Si occurred while no such effects were detected in the Mo $4p$ spectrum even at the largest exposure investigated. The surface-shifted components were extracted using a curve-fitting procedure and for the (110) surface one shifted component was found to produce fairly good fits while for the (100) surface two shifted components were found to be needed in order to model the experimental results. For the (100) surface the major component exhibited a surface shift of $-0.68(2)$ eV and the minor (having about 10% of the intensity of the major component) a shift of $-1.03(4)$ eV. For the (110) surface the surface shift was found to be $-1.02(1)$ eV. The partial shift originating from the loss of coordination at the surface has been used as an estimate of the surface core level. A negative surface shift is predicted for both surfaces and if perfect bulk termination is assumed the shift on the (110) surface is expected to be 50% larger than on the (100) surface. The magnitude of this predicted partial shift is, however, less than half of the observed shift and therefore speculations about other contributions have been presented. The experimental results suggest that the surfaces may be Si terminated but the amount of Si in the surface layer could not be determined although the surface-to-bulk intensity ratios were extracted both as a function of photon energy and electron emission angle. These ratios are presented and shown to be dominated by diffraction effects, which explains why the commonly used simple model to estimate the amount of "surface coverage" is not applicable in this case. The strong diffraction effects do instead open up possibilities for extracting valuable

structural information. Presently, however, we cannot augment these experimental findings with multiple-scattering calculations to extract the structural information contained in the data. That will be the challenge for future investigations.

ACKNOWLEDGMENTS

The authors would like to thank the staff at the MAX laboratory for their support during the experiments and the Swedish Natural Science Research Council for their financial support.

- *Permanent address: Interdisciplinary Research Centre in Surface Science and Department of Chemistry, University of Manchester, Manchester M13 9PL, United Kingdom.
- ¹S. P. Murarka, *Silicides for VLSI Application* (Academic, New York, 1983).
- ²C. Calandra, O. Bisi, and G. Ottovani, *Surf. Sci. Rep.* **4**, 273 (1985), and references therein.
- ³T. T. A. Nguyen and R. C. Cinti, *J. Phys. (Paris) Colloq.* **C5**, 435 (1984).
- ⁴H. Balaska, R. C. Cinti, T. T. A. Nguyen, and J. Derrien, *Surf. Sci.* **168**, 225 (1986).
- ⁵G. Rossi, I. Abbati, L. Braichovich, I. Lindau, and W. E. Spicer, *J. Vac. Sci. Technol.* **21**, 617 (1982).
- ⁶G. Rossi, I. Abbati, L. Braichovich, I. Lindau, W. E. Spicer, U. del Pennino, and S. Nannarone, *Physica B+C* **117-118B**, 795 (1983).
- ⁷I. Abbati, L. Braichovich, B. de Michelis, A. Fasana, and A. Rizzi, *Surf. Sci.* **177**, L901 (1986).
- ⁸T. T. A. Nguyen, M. Azizan, R. C. Cinti, G. Chauvet, and R. Baptist, *Surf. Sci.* **162**, 651 (1985).
- ⁹J. H. Weaver, V. L. Moruzzi, and F. A. Schmidt, *Phys. Rev. B* **23**, 2916 (1981).
- ¹⁰T. Komeda, T. Hirano, G. D. Waddill, S. G. Anderson, J. P. Sullivan, and J. H. Weaver, *Phys. Rev. B* **41**, 8345 (1990).
- ¹¹K. L. Håkansson, L. I. Johansson, P. E. S. Persson, P. L. Wincott, and A. N. Christensen (unpublished).
- ¹²U. O. Karlsson, J. N. Andersen, K. Hansen, and R. Nyholm, *Nucl. Instrum. Methods A* **282**, 533 (1989).
- ¹³A. N. Christensen, *Acta Chem. Scand. A* **37**, 519 (1983).
- ¹⁴P. H. Mahowald, D. J. Friedman, G. P. Carey, K. A. Bertness, and J. J. Yeh, *J. Vac. Sci. Technol. A* **5**, 2982 (1987).
- ¹⁵G. Hollinger and F. J. Himpsel, *J. Vac. Sci. Technol. A* **1**, 640 (1983); F. J. Himpsel, F. R. McFeely, A. Taleb-Ibrahimi, J. A. Yarmoff, and G. Hollinger, *Phys. Rev. B* **38**, 6084 (1988).
- ¹⁶G. Zajak, J. Zak, and S. D. Bader, *Phys. Rev. B* **27**, 6649 (1983).
- ¹⁷M. P. Seah and W. A. Dench, *Surf. Interface Anal.* **1**, 2 (1979).
- ¹⁸J. F. Morar, U. O. Karlsson, J. A. Yarmoff, D. Riegler, F. R. McFeely, and F. J. Himpsel (unpublished).
- ¹⁹T. Miller, A. P. Shapiro, and T. C. Chiang, *Phys. Rev. B* **31**, 7915 (1985).
- ²⁰A. Nilsson, B. Eriksson, N. Mårtensson, J. N. Andersen, and J. Onsgaard, *Phys. Rev. B* **38**, 10 357 (1988), and references therein.
- ²¹*Cohesion in Metals*, edited by F. R. deBoer and D. G. Pettifor (North-Holland, Amsterdam, 1988), Vol. 1, Chap. IV.
- ²²See Chap. III in Ref. 21.
- ²³R. Leckey, J. D. Riley, R. L. Johnson, L. Ley, and B. Ditchek, *J. Vac. Sci. Technol. A* **6**, 63 (1988).
- ²⁴H. C. Poon, G. Grenet, S. Holmberg, Y. Jugnet, Tran Minh Duc, and R. Leckey, *Phys. Rev. B* **41**, 12 735 (1990).
- ²⁵J. E. Rowe, G. K. Wertheim, and R. T. Tung, *J. Vac. Sci. Technol. A* **7**, 2454 (1989).
- ²⁶Y. Jugnet, N. S. Prakash, L. Porte, Tran Minh Duc, T. T. Nguyen, R. Cinti, H. C. Poon, and G. Grenet, *Phys. Rev. B* **37**, 8066 (1988).
- ²⁷R. A. Bartynski, D. Heskett, K. Garrison, G. Watson, D. M. Zehner, W. N. Mei, S. Y. Tong, and X. Pan, *J. Vac. Sci. Technol. A* **7**, 1931 (1989).